The melting temperature of the most common models of water

C. Vega, E. Sanz, and J. L. F. Abascal
Departmento de Química Física, Facultad de Ciencias Químicas, Universidad Complutense, 28040 Madrid, Spain

(Received 29 November 2004; accepted 4 January 2005; published online 21 March 2005)

The melting temperature of ice I_h for several commonly used models of water (SPC, SPC/E,TIP3P,TIP4P, TIP4P/Ew, and TIP5P) is obtained from computer simulations at $p=1$ bar. Since the melting temperature of ice I_h for the TIP4P model is now known [E. Sanz, C. Vega, J. L. F. Abascal, and L. G. MacDowell, Phys. Rev. Lett. **92**, 255701 (2004)], it is possible to use the Gibbs–Duhem methodology [D. Kofke, J. Chem. Phys. **98**, 4149 (1993)] to evaluate the melting temperature of ice I_h for other potential models of water. We have found that the melting temperatures of ice I_h for SPC, SPC/E, TIP3P, TIP4P, TIP4P/Ew, and TIP5P models are $T=190$ K, 215 K, 146 K, 232 K, 245 K, and 274 K, respectively. The relative stability of ice I_h with respect to ice II for these models has also been considered. It turns out that for SPC, SPC/E, TIP3P, and TIP5P the stable phase at the normal melting point is ice II (so that ice I_h is not a thermodynamically stable phase for these models). For TIP4P and TIP4P/Ew, ice I_h is the stable solid phase at the standard melting point. The location of the negative charge along the H–O–H bisector appears as a critical factor in the determination of the relative stability between the I_h and II ice forms. The methodology proposed in this paper can be used to investigate the effect upon a coexistence line due to a change in the potential parameters. © *2005 American Institute of Physics*. [DOI: 10.1063/1.1862245]

I. INTRODUCTION

Water is probably the most important molecule in our relation to nature. It forms the matrix of life,[1] it is the most common solvent for chemical processes, it plays a major role in the determination of the climate on earth, and also it appears on planets, moons, and comets.[2] More than 30 years ago, computer simulations of water started their road with the pioneering papers by Watts and Barker[3] and by Rahman and Stillinger.[4] A key issue when performing simulations of water is the choice of the potential model used to describe the interaction between molecules.[5–9] A number of different potential models have been proposed (see Ref. 10 for a comprehensive review). It is probably fair to say that the potentials for water most commonly used in the past years have been the SPC,[11] SPC/E,[12] TIP3P,[13] and TIP4P (Ref. 13). models. Two recently proposed models, namely, TIP5P (Ref. 14) and TIP4P/Ew,[15] also give promising results and are increasingly used nowadays. The potential parameters of these models were often chosen to reproduce thermodynamic and/or structural[16,17] properties of water at room temperature and pressure. A naive question arises naturally: are the simple models of water used so far able to provide a reasonable description of the phase diagram of water?

The vapor-liquid equilibria and supercritical properties of the most common models of water are now well known.[10,18–26] The phase equilibria of supercooled water has been an active area of experimental[27–36] and computational[37–43] research in the last two decades. Somewhat surprisingly, the solid-solid and fluid-solid equilibria have received much less attention. In fact, the number of simulations studies of ice phases is rather limited[44–48] and the fluid-solid equilibria has been considered by a relatively small number of researchers such as Tanaka and co-workers,[49] van der Eerden and co-workers,[50,51] Clancy and co-workers,[52,53] Haymet co-workers,[54,55] and Woo and Monson.[56] In the majority of these studies (being Refs. 52 and 56 the only exceptions) only the melting of ice I_h and/or ice Ic was considered even though water presents one of the richest phase diagrams. In fact, the phase diagram of water[57–60] presents (at least) 13 different solid phases,[58] the last one discovered just a few years ago by Lobban, Finney, and Kuhs[61] and analyzed in more detail in the last few years.[62,63]

Recently, we have undertaken the goal of determining the phase diagram of water for the simple SPC/E and TIP4P models.[64–68] This is a rather involved task since since it requires several steps. First, it is necessary to calculate the free energies for the solid phases for which we used the Frenkel–Ladd method.[69,70] Due to the fact that some ice phases (ice III and ice V) present not total proton disorder but rather partial proton disorder,[71] a methodology to determine such a disorder entropy is needed. To this end, we extended[66] the ideas of Howe and Whitworth.[72] Then, we performed isobaric-isothermal Monte Carlo simulations (*N*-*p*-*T*) using Parrinello–Rahman sampling[73] for the fluid and solid phases to calculate the point at which the chemical potentials and pressures of the phases of interest are equal. The Gibbs–Duhem integration first proposed by Kofke[74–78] allows one to determine the full coexistence line provided that an initial coexistence point is known. In our previous work we have used this methodology to determine the coexistence lines between different phases and to plot for the first time the phase diagram of two simple models of water. However, Kofke soon noticed after his proposal of the Gibbs–Duhem method[79,80] that the method could be used not only to get

coexistence lines (i.e., the change in the coexistence pressure with temperature) but also in an apparently different way. In fact, Gibbs–Duhem integration can be used to determine the unknown coexistence point of a given potential model provided that the coexistence point for a different potential is known. This methodology has already been used by several groups[81–83] to study the evolution of a certain coexistence line when the potential model is changed.

When performing simulations of water, it is interesting to know the exact location of the normal melting temperature of the model. Thus, an interesting application of the Gibbs–Duhem technique would be the determination of the melting point temperature at room pressure for the most popular models of water. In this work we use such methodology to determine the melting point of some popular models of water, namely, SPC, TIP3P, TIP5P, and TIP4P/Ew from the known melting point temperatures of SPC/E and TIP4P. The water-ice I_h coexistence temperatures at $p=1$ bar will be provided. We will also analyze whether ice I_h is indeed the stable solid phase at room pressure or if, eventually, ice II becomes more stable. The technique proposed here allows one to determine, in a relatively straightforward way, the effect that a certain change in the parameters of the potential has upon the melting temperature, or more generally on a given phase transition, indicating clearly which parameters should be changed within a certain geometry to improve the agreement with experiment. Sec. II describes the models and methodology used in this work. Section III presents the results for the melting lines and the relative stability of ices I_h and II for different water potential models. The papers ends with a final discussion and the conclusions of this work.

II. MODELS AND METHODS

A. Hamiltonian Gibbs–Duhem integration

Let us denote G, V, S, H the thermodynamic properties per particle. In the isobaric isothermal ensemble (N-p-T), once integration over momenta space is performed, the Gibbs free energy can be written as

$$NG(p,T,\lambda) = -kT \ln \frac{q^N}{N!} \int \exp(-\beta pV) \times \left[\int \exp(-\beta U(\lambda)) d1 \cdots dN \right] dV, \quad (1)$$

where we have assumed that—in addition to the coordinates of the molecules—the energy of the system U depends parametrically on a variable denoted as λ. As usual, $\beta=1/(k_BT)$ and q is the partition function containing electronic and vibrational degrees of freedom and the contribution obtained after integration over translational and rotational momenta. We can use λ as a new intensive thermodynamic variable so that a change in Gibbs free energy per particle is given by

$$dG = -S\,dT + V\,dp + X_G d\lambda, \quad (2)$$

where the conjugate thermodynamic variable X_G is

$$X_G = \left(\frac{\partial G}{\partial \lambda} \right)_{p,T}. \quad (3)$$

Thus,

$$NX_G = \frac{\int \exp(-\beta pV) \left[\int (\partial U(\lambda)/\partial \lambda) \exp(-\beta U(\lambda)) d1 \cdots dN \right] dV}{\int \exp(-\beta pV) \left[\int \exp(-\beta U(\lambda)) d1 \cdots dN \right] dV}, \quad (4)$$

and, finally,

$$NX_G = \left\langle \frac{\partial U(\lambda)}{\partial \lambda} \right\rangle_{N,p,T,\lambda} \quad (5)$$

Let us assume that two phases—labeled with subscripts 1 and 2—are in equilibrium for a system of only one component. The condition of equilibrium is satisfied at a certain T and p whenever $G_1=G_2$. If the system is now perturbated in such a way that the phases are still in equilibrium, it must hold that $dG_1=dG_2$. There are several ways of perturbating the system. If this is done by keeping λ constant (i.e., without changing the Hamiltonian of the system), one obtains

$$-S_1 dT + V_1 dp = -S_2 dT + V_2 dp, \quad (6)$$

and, rearranging terms

$$\frac{dp}{dT} = \frac{S_2 - S_1}{V_2 - V_1} = \frac{H_2 - H_1}{T(V_2 - V_1)}, \quad (7)$$

which is the well known Clapeyron equation. The integration of this differential equation, using computer simulations to estimate the properties on the right hand side, will be denoted as *thermodynamic* Gibbs–Duhem integration. Incidentally, it should be noted that, when dealing with the melting lines of ices, it is sometimes numerically more convenient to integrate the corresponding Clapeyron equation for dT/dp:

$$\frac{dT}{dp} = \frac{T(V_2 - V_1)}{H_2 - H_1}. \quad (8)$$

However other perturbations are possible. For instance one may perturbate the system by changing λ while keeping p constant. In that case, it holds

$$-S_1 dT + X_{G,1} d\lambda = -S_2 dT + X_{G,2} d\lambda, \quad (9)$$

which leads to a generalized Clapeyron equation

TABLE I. Potential parameters of the water potential models used in this work. The distance between the oxygen and hydrogen sites is d_{OH}. The angle formed by hydrogen, oxygen, and the other hydrogen atom is denoted as H–O–H. The LJ site is located on the oxygen with parameters σ and ϵ/k. The charge on the proton is q_H. All the models (but TIP5P) place the negative charge in a point M at a distance d_{OM} from the oxygen along the H–O–H bisector. For TIP5P, d_{OL} is the distance between the oxygen and the sites L placed at the lone electron pairs (the angle L–O–L is the tetrahedral angle 109.47).

Model	d_{OH} (Å)	H–O–H	σ (Å)	(ϵ/k) (K)	q_H (e)	d_{OM} (Å)	d_{OL} (Å)
SPC	1.0	109.47	3.1656	78.20	0.41	0	⋯
SPC/E	1.0	109.47	3.1656	78.20	0.423 8	0	⋯
TIP3P	0.9572	104.52	3.1506	76.54	0.417	0	⋯
TIP4P	0.9572	104.52	3.1540	78.02	0.52	0.15	⋯
TIP4P/Ew	0.9572	104.52	3.1643	81.90	0.524 22	0.1250	⋯
TIP5P	0.9572	104.52	3.1200	80.51	0.241	⋯	0.70

$$\frac{dT}{d\lambda} = \frac{T(X_{G,2} - X_{G,1})}{H_2 - H_1}. \tag{10}$$

This equation shows how the coexistence temperature T changes when λ is modified while keeping constant the pressure. The integration of this differential equation by using computer simulations to estimate the terms on the right-hand side will be denoted here as constant pressure Hamiltonian Gibbs–Duhem integration. Finally, one may be interested in analyzing the change in the coexistence pressure with λ while keeping T constant. In this case the generalized equation Clapeyron is

$$\frac{dp}{d\lambda} = -\frac{(X_{G,2} - X_{G,1})}{V_2 - V_1}, \tag{11}$$

which is the basis of the procedure here referred to as constant temperature Hamiltonian Gibbs–Duhem integration.

Let us now apply the previous equation to the particular case of a system for which the interaction energy is pairwise additive,

$$U = \sum_{i<j} \sum u_{ij}, \tag{12}$$

where $u(i,j)$ is the interaction between molecule i and molecule j. We also assume that the pair interaction may be split as

$$u = (1 - \lambda)u_{ref} + \lambda u_{new}, \tag{13}$$

where, for simplicity, we drop the subindices i and j. In the above equation, u_{ref} is a reference potential for which the coexistence properties are known and u_{new} is the pair potential for which we would like to know the coexistence properties. When $\lambda = 0$, u becomes the reference system pair potential whereas, for $\lambda = 1$, it becomes that of the new system. In this case, X_G is given by

$$NX_G = \langle U_{new} - U_{ref} \rangle, \tag{14}$$

where the bracket denotes ensemble average over a system interacting through Eq. (13) at a certain value of λ. Equations (10) and (11) are differential equations that can be integrated from $\lambda = 0$ with coexistence properties $p = p_0$, $T = T_0$ to $\lambda = 1$. In this way, the coexistence properties of the new model can be determined from those of the reference model using the Hamiltonian Gibbs–Duhem integration. It should be noted that, for the procedure to be valid, none of the coexistence phases should undergo a phase transition along the integration line.

B. Water models

In Table I the geometry and the potential parameters of several popular potential models for water are presented. All these models have two common features: a Lennard–Jones (LJ) center is located on the oxygen atom and positive charges are situated on the hydrogen atoms.

In the TIPs models of Jorgensen *et al.*[13] the experimental values of the O–H bond length and H–O–H bond angle are used. Differences between the different TIP models arises from the location of the negative charge. In the TIP3P model the negative charge is located on the oxygen atom. In the TIP4P model the negative charge is located on a point M which is placed at a distance d_{OM} from the oxygen along the H–O–H bisector in the direction of the positive charges as first suggested by Bernal and Fowler.[84] A new version of TIP4P, with potential parameters optimized for Ewald sums (instead of the simple truncation of the potential used in the original TIP4P) has been proposed by Horn *et al.*[15] This model is denoted as TIP4P/Ew. In the TIP5P model[14] two partial charges are placed at the positions of the "lone electron pairs." The geometry of the TIP5P is similar to that of the water models of the 1970s as, for instance, ST2.[85]

In the SPC model, first proposed by Berendsen *et al.*,[12] the geometry of the molecule does not correspond to the experimental one. The O–H bond length is assigned to 1 Å and the H–O–H bond angle is set to the tetrahedral value. The negative charge are located at the position of the oxygen atom. In 1987, Berendsen *et al.*[12] suggested that the polarization energy should be added to the internal energy of the liquid when fitting the potential parameters of the model to the vaporization enthalpy of real water. In this way Berendsen proposed a new water potential denoted as SPC/E. The geometry is the same as that of SPC, but the partial charges on H and O atoms are increased slightly.

When using Eq. (13), it should be clearly stated how the "mixed" potential is defined, in particular, how the "reference" and "new" potentials are linked geometrically. In this work the position of the O atom is the same in both potentials. The H–O–H bisector is also the same and we impose

that in both models the atoms of the molecule remain in the same plane. These three conditions determine in a unique way how u_{ref} and u_{new} are "connected" geometrically. Notice that there is no crossed interaction between the sites of u_{ref} and those of u_{new}.

C. Simulation details

In our simulations, the LJ potential was truncated for all phases at 8.5 Å. Standard long range corrections to the LJ energy were added. The importance of an adequate treatment of the long range coulombic forces when dealing with water simulations has been pointed out in recent studies.[86–88] leading to new set of potential parameters.[88–90] In this work, the Ewald summation technique[91] has been employed for the calculation of the long range electrostatic forces. The number of particles for the liquid, ice I_h and ice II were 360, 288 and 432, respectively. Isotropic N-p-T simulations were used for the liquid phase while anisotropic Monte Carlo simulations (Parrinello–Rahman like[73,92]) were used for the solid phases. To integrate the generalized Clapeyron equation, which is a first-order differential equation, a fourth order Runge–Kutta integration algorithm was used. Four to eight values of λ were used to go from the reference potential to the final potential. The initial coexistence properties for $\lambda=0$ (i.e., the reference system) must be known. The TIP4P and/or the SPC/E model were used as reference systems because their coexistence lines are now well known.[64,65] Typically, about 20 000 cycles were used for determining the properties of each phase for a given state (a cycle is defined as a trial move per particle plus a trial volume change).

Initial configurations were prepared as follows. For the disordered phase I_h, we used the algorithm of Buch *et al.*[93] to generate a starting configuration having no net dipole moment and where the hydrogens (but not the oxygens) are disordered and satisfy the ice rules.[84,94] Other algorithms to generate disordered configurations in ice are also available.[95] Ice II is proton ordered, so we used crystallographic information to generate an initial solid configuration.[96]

III. RESULTS

The fluid-solid coexistence temperatures at $p=1$ bar for TIP4P and SPC/E have been determined recently[64,65] by performing free energy calculations. Their values are $T=232\pm5$ K and $T=215\pm5$ K, respectively. These numbers are in relatively good agreement with previous calculations for TIP4P, namely, $T=238\pm7$ K,[49] $T=229$ K,[97] and for SPC/E, $T=225\pm5$ K.[54,55] Starting from the SPC/E model and performing constant pressure Hamiltonian Gibbs–Duhem simulations (integrating the generalized Clapeyron equation as described in the preceding section) one should recover the melting temperature of the TIP4P. The results of this check are presented in Table II. Starting from the SPC/E ice I_h melting point we obtain $T=232.3$ K for TIP4P, in very good agreement with the result obtained through free energy calculations. The results presented in Table II constitute a cross-check not only of the Gibbs–Duhem methodology proposed here but also of the free energy calculations of our previous work.[64,65] Appliying this methodology the melting temperature of the SPC has been determined. For the SPC the melting temperature (see Table II) was found to be 190 K, more than 80° below the experimental value $T=273.15$ K. For the TIP5P we take as an initial reference systems both the SPC/E and the TIP4P potentials. Obviously, the properties of the final model should be independent of the reference model. When the starting model is SPC/E we obtain $T=275$ K for TIP5P whereas the calculated result using the TIP4P model as a reference is $T=273$ K. The agreement between both estimates is satisfactory taking into account that the error of the Gibbs-Duhem integration is about 3 K. We conclude that the melting point of ice I_h for the TIP5P model is $T=274\pm3$ K, in quite good agreement with experiment. For TIP5P, Nada and van der Eerden[51] have reported a melting temperature of $T=274$ K and recently Koyama *et al.*[97] reported $T=268$ K. Thus, our results are again in good agreement with bibliographic data. The last two models considered in this work are the TIP3P and the TIP4P/Ew. We used the TIP4P as reference system to the determine the melting temperature of ice I_h at $p=1$ bar. We obtained $T=146$ K for the TIP3P model and $T=245.5$ K for the TIP4P/Ew.

TABLE II. Liquid-ice I_h coexistence at $p=1$ bar for TIP4P and SPC from constant pressure Hamiltonian Gibbs–Duhem integration starting from the SPC/E model.

T (K)	λ	Model
	From SPC/E to TIP4P	
215.0	0	SPC/E
227.8	0.5	⋯
232.3	1	TIP4P
	From SPC/E to SPC	
215.0	0	SPC/E
198.5	0.6667	⋯
190.4	1	SPC

Table III presents the melting properties of ice I_h for the models considered in this work. Relatively long runs (with 800 000 cycles) were performed to precisely determine the properties of the fluid and solid phase at the coexistence conditions. All the models but TIP5P yield too low melting temperatures. Departures from the experimental data are larger than 25 K in all cases with the noticeable exception of TIP5P which essentially matches the experimental value. Concerning the melting enthalpies, the predictions of SPC, SPC/E, and TIP3P are too low by a factor of 2 or 3. TIP4P and TIP4P/Ew yield values which are about 0.4 Kcal/mol below the experimental one. Again, the behavior of TIP5P differs from that of the rest of the models as it overestimates the melting enthalpy (by 0.35 Kcal/mol). As to the density of I_h at coexistence, it is overestimated by all the models. However, the agreement is reasonable for SPC, TIP4P, and TIP4P/Ew. The SPC/E prediction is less good and the departure of the TIP5P result from experiment is quite significant (over a 5%). Note that, for liquid water, the agreement is acceptable in all cases. This is not a surprise since these are "liquid water" potentials. Let us now compare the slope of the coexistence curve dp/dT. SPC and SPC/E show a fair

TABLE III. Melting properties of ice I_h at $p=1$ bar for different models. T_m and T_c, melting and critical temperatures; ρ_l and ρ_{I_h}, coexistence densities of liquid water and ice; H_l and H_{Ih}, enthalpies of liquid and ice (we have not included the $3RT$ term arising from the translational and rotational kinetic terms); ΔH, melting enthalpy; dp/dT, slope of the coexistence curve. Numbers in parenthesis for the TIP4P model are the estimated errors for TIP4P. The errors for the other models are of the same order of magnitude. Unless otherwise stated, the quantities have been calculated in this work.

Model	SPC	SPC/E	TIP4P	TIP4P/Ew	TIP5P	TIP5P[a]	TIP3P	Expt.
T_m (K)	190.5	215	232.(5)	245.5	273.9	270	145.6	273.15
T_c (K)[b]	593.8	638.6	588.2	⋯	521.3	521.3		647.1
T_m/T_c	0.321	0.337	0.394	⋯	0.525	0.517		0.422
ρ_l (g/cm^3)	0.991	1.011	1.002(6)	0.992	0.987	1.000	1.017	0.999
ρ_{Ih} (g/cm^3)	0.934	0.950	0.940(2)	0.936	0.967	0.982	0.947	0.917
H_l (Kcal/mol)	−11.64	−12.49	−10.98	−12.02	−10.33	⋯	−11.69	⋯
H_{Ih} (Kcal/mol)	−12.22	−13.23	−12.03	−13.07	−12.08	⋯	−11.99	⋯
ΔH (Kcal/mol)	0.62	0.74	1.05(5)	1.05	1.75	1.73	0.3	1.44
dp/dT (bar/K)	−115	−126	−160(20)	−164	−708	−714	−66	−135

[a]From Ref. 51.
[b]From Ref. 22 (SPC, SPC/E), Ref. 23 (TIP4P), Refs. 87 and 99 (TIP5P).

agreement with the experimental value. The slope of TIP4P and TIP4P/Ew are somewhat high and that of TIP5P is wrong by a factor of 5. The reason of this large slope for the TIP5P model is the very small density change between ice I_h and water at melting for this model.[51,97] Note that, our results for TIP5P are in reasonable agreement with those of Nada and van der Eerden.[51] The balance of the results presented so far is that the geometry of the TIP4P model seems to be superior to that of SPC and TIP5P, at least concerning the melting properties of ice I_h. TIP4P/Ew seems also an acceptable model to study freezing or melting of ice I_h. The critical temperature of these models has been recently determined by applying the Gibbs ensemble technique[98] to water.[22,23,87,99] Thus, it is interesting to analyze the liquid range of these models as determined by the ratio of the melting T_m to the critical temperature T_c. This ratio is also presented in Table III. Values of T_m/T_c are quite low for SPC and SPC/E models, too high for TIP5P, and for TIP4P are closer to the experimental results.

So far we have computed the melting temperature of ice I_h at $p=1$ bar for different water models. However, it is not obvious at all if among all solid phases of water, ice I_h is indeed the most stable one at these conditions for the water models considered in this work. Likely, ice II is the competing phase of ice I_h for any reasonable water model, and the relative stability between these two phases determines whether or not ice I_h is a stable phase for a given model. We address this issue by using the generalized Gibbs–Duhem integration to a solid-solid equilibrium. In this case, we perform constant temperature Hamiltonian Gibbs–Duhem integration rather than the constant pressure version used previously in this work. The I_h-II coexistence pressure at $T=150$ K for TIP4P is $p=3041$ bars. From this point we have computed the coexistence pressure at the same temperature for SPC, SPC/E, TIP3P, TIP5P, and TIP4P/Ew (in this last model for $T=180$ K). The results are presented in Table IV. For both SPC/E and TIP5P the coexistence pressure at $T=150$ K occurs at a pressure of about −500 bars, being somewhat lower for SPC (−948 bars) and much lower for the TIP3P. Ice II is the stable phase at higher pressures and ice I_h for lower pressures. Besides, the slope of the I_h-II coexistence curve is very small (6 bar/K for SPC/E and −0.9 bar/K for TIP5P). This suggests that ice I_h is not a thermodynamically stable phase at positive pressures neither for the SPC/E model (as shown previously[64,65]) nor for SPC, TIP3P and TIP5P models as shown in this work. It seems that if the negative charge of a water model is located either at the oxygen atom (as in SPC, SPC/E, or TIP3P models) or at the lone electron pairs (as in TIP5P) ice II becomes more stable than ice I_h. Ice I_h is stable with respect to ice II only when the negative charge is located on the H–O–H bisector in the direction of the hydrogen atoms. This is in agreement

TABLE IV. Ice I_h-II coexistence at $T=150$ K obtained from constant temperature Gibbs–Duhem integration. Results in the upper part correspond to the integration from TIP4P to SPC/E and from TIP4P to SPC. Results in the middle part correspond to the integration from the TIP4P to the TIP3P model and from TIP4P to the TIP5P model. Results in the bottom correspond to the integration from the TIP4P to the TIP4P/Ew model at $T=180$ K.

Model	T (K)	p (bar)	λ
TIP4P	150	3041	0.0000
	150	1077	0.5000
SPC/E	150	−498	1.0000
TIP4P	150	3041	0.0000
	150	774	0.5000
SPC	150	−948	1.0000
TIP4P	150	3041	0.0
	150	−583	0.5
TIP3P	150	−3395	1.0
TIP4P	150	3041	0.
	150	1463	0.5
TIP5P	150	−587	1.0
TIP4P	180	3173	0.0
	180	2672	0.5
TIP4P/Ew	180	2198	1.0

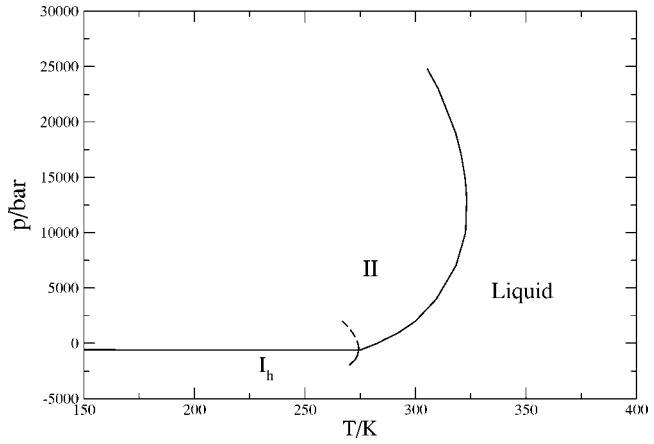

FIG. 1. Phase diagram of the TIP5P model when liquid water ice I_h and ice II are considered. Lines were obtained from conventional Gibbs–Duhem simulations.

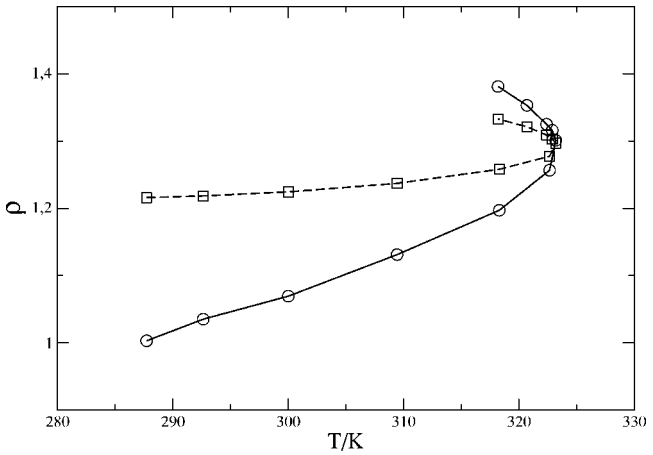

FIG. 2. Densities at equilibrium for the water-ice II coexistence curve of the TIP5P model (in g/cm^3). The equilibrium coexistence densities are plotted as a function of the coexistence temperature. Open circles and solid lines: coexistence densities of water. Open squares and dashed lines: coexistence densities of ice II.

with results from quantum chemistry.[100] and probably hinted at by several authors[101,102] starting from Bernal and Fowler,[84] who proposed the first water model.

In Fig. 1 the phase diagram of the TIP5P is presented (we only considered ice I_h, water and ice II) obtained by conventional Gibbs–Duhem integration. Note the presence of reentrant melting for ice II (i.e., the existence of a maxima in the melting temperature when plotted as a function of pressure) and also for ice I_h (in this case the change of sign in the slope of the dp/dT curve occurs at negative pressures). The explanation for the existence of reentrant melting was discussed previously[64] and is due to he higher compressibility of liquid water with respect to the "low dense" ice phases (I–VI). Tammann after studying the melting curves of ice (I, III) suggested that the melting curves of all substances should present melting maxima (as quoted by Bridgman in Ref. 57). Stishov in the sixties showed the existence of melting maxima for Tellurium and Cesium.[103,104] Other substances such as carbon (graphite) and silica (SiO_2) also seem to present melting maxima[105,106] (i.e., a reentrant melting curve). Our simulations results from this and previous work[64,65] show clearly the existence of melting maxima for ices with relatively low density (I_h–VI) and its absence for high density ices (VII and VIII). Although Tammann was not right in stating that all melting curves present melting maxima, he was not completely wrong either: some substances such as Te, Cs, and water exhibit this maxima (although for real water the melting maxima seems to appear in the metastable region of the melting curve). In Fig. 2 the origin of this melting maxima is clarified. In this figure the coexistence densities for ice II and water along the melting curve are plotted. At low pressures the density of ice II at coexistence is higher than that of water, whereas the opposite is true at high pressures. This is due to the higher compressibility of water when compared to that of ice II. The volume change at melting goes from positive (low pressures) to negative values (high pressures). Since the melting enthalpy is always positive that means (from the Clapeyron equation) that the slope of the dp/dT curve goes from positive (low pressures) to negative values (high pressures). As can be seen the change of slope of the melting curve in the p-T representation occurs at the temperature for which the coexistence densities of ice II and water become identical. Notice that melting is still a first-order phase transition there since the entropy change (i.e, the melting enthalpy) is different from zero even though the volume change is zero.[70,107] The results of Figs. 1 and 2 illustrate the origin of the big value of dp/dT for the liquid-I_h transition at $p=1$ bar found for the TIP5P model (see Table III). The small density change at melting for the TIP5P model is due to the proximity of a reentrant point in the liquid-I_h coexistence curve, which occurs at about $p=-600$ bars, and at which the density of both phases become identical yielding an infinite value for the slope of the dp/dT curve. In summary the large slope of dp/dT at $p=1$ bar for TIP5P is due to the proximity of a reentrant point occurring at slightly negative pressures (for the TIP4P the reentrant point also exists but it is located at more negative pressures, i.e., about −1500 bars very close to the location estimated from extrapolation of experimental measurements[108]).

The Hamiltonian Gibbs–Duhem integration can be used to evaluate the impact of a change of a parameter of the potential on a certain coexistence curve. If the geometry of the TIP4P model is kept fixed (bond lengths and angles) then the TIP4P model is defined by the magnitude of the charge located on the H atom q_H/e, by the distance d_{OM} of the negative charge from the oxygen atom along the H–O–H bisector, and by the Lennard–Jones parameters σ and ϵ. We decided to increase the magnitude of the proton charge by $0.03e$, the distance d_{OM} by 0.03 Å, the value of ϵ/k by 6 K, and the value of σ by 0.026 Å (only one parameter was changed each time) to evaluate its impact on the melting point. Since the change of the potential parameter is small we can estimate approximately the rate of change of the melting temperature with the potential parameter as

$$T_X = \frac{dT_m}{dX} = \frac{\Delta T_m}{\Delta X}, \tag{15}$$

where ΔT_m is the change in the coexistence temperature at a certain pressure and ΔX is the change in the potential param-

eter $X=(\epsilon/k)$ (K), σ (Å), d_{OM} (Å), q_{H} (e). The change in .the parameter should be sufficiently small to approximate a derivative by an incremental ratio, but not too small since in this case ΔT_m will be of the same order of magnitude of our numerical uncertainty and we could not evaluate the derivative properly. We obtained the following values for the water-I_h TIP4P coexistence curve, $T_{q\mathrm{H}}=1462.27$ K, $T_{\epsilon}=-1.7645$ K, $T_{\sigma}=-504.008$ K, and $T_{d_{\mathrm{OM}}}=-810.76$ K. According to this an increase of q_{H} increases the melting temperature of ice I_h, however an increase in σ, ϵ, or d_{OM} provokes a decrease of the melting temperature of ice I_h. The effect of a change of the potential parameter on the melting temperature is not always obvious. One could guess some changes (but not all). For instance one could imagine that increasing the H charge will make the solid more stable with respect to the liquid since that increases the hydrogen bonding energy. Also increasing d_{OM} makes the charge distribution less favorable for hydrogen bonding, doing the solid less stable. Increasing ϵ seems to stabilize the phase with higher van der Waals energy which is typically the more dense phase. For this reason increasing (ϵ/k) (K) makes liquid water more stable than ice. More surprising is the effect of σ. One would expect that increasing σ makes the more dense phase less stable. However the opposite is true. Note that in ice I_h the oxygen-oxygen nearest neighbors distance is shorter than in the liquid, and for this reason, ice I_h and not water is more strongly destabilized by an increase of σ.

IV. CONCLUSIONS

In this paper we show that the Gibbs–Duhem methodology can be used to calculate the melting temperature of a certain water potential starting from the known melting temperature of a distinct water model. The melting temperature of ice I_h—recently determined for the TIP4P and SPC/E models by computing the free energies of the fluid and solid phases[64,65]—is used as initial reference state. In this way the melting properties of the TIP3P, TIP4P/Ew, TIP5P, and SPC models was calculated. It turns out that the melting temperature at $p=1$ bar of all of the water models calculated so far (with the exception of the TIP5P model) are below the experimental value. None of the models give acceptable predictions for all the melting properties. However, in the overall, the results for TIP4P and TIP4P/Ew are well balanced and are the best models for the study of the melting of ice I_h. The TIP4P predictions of the complete phase diagram are also quite acceptable[64,65] so this model is a good candidate for the investigation not only of ice I_h but also of other solid forms of water. Notice also that a knowledge of the melting temperature is required for studies of ice nucleation in supercooled water,[109–111] crystal growth,[112] or freezing (phase transitions) of water in nanopores.[113–115]

In a second application of the Gibbs–Duhem methodology, we have computed the I_h-II coexistence pressure at $T=150$ K for the water models considered in this work. It turns out that the coexistence pressure moves to negative values for the SPC, SPC/E, TIP3P, and TIP5P models and remains positive for TIP4P and TIP4P/Ew models. As a consequence, ice I_h does not appear in the phase diagram of SPC, SPC/E, TIP3P, and TIP5P and is stable only at negative pressures. The thermodynamic stability should not be confused with the mechanical stability.[68,116] For SPC, SPC/E, and TIP5P, it is possible to perform simulations of ice I_h at moderate (positive) pressures and the results correspond to that of a mechanically stable solid structure. However, at those conditions, there is always another ice phase (ice II) with lower Gibbs free energy so that I_h is not thermodynamically stable. Only for the TIP4P and TIP4P/Ew ice I_h appears as a thermodynamically stable phase. In our opinion all these results point in a clear direction: the center of the negative charge in real water is located along the H–O–H bisector in the direction of the hydrogen atoms. All the attempts to locate the negative charge either at the oxygen (SPC, SPC/E, and TIP3P) or at the lone electron pairs (TIP5P) yield models in which ice II is far more stable than ice I_h, in clear disagreement with experiment. The idea of locating most of the negative charge in water along the lone electron pairs stems from the old fashioned idea of hybrid orbitals. Neither quantum chemistry calculations[58,100] nor the results of this work support the idea of locating most of the negative charge of the water model on the lone pairs electrons.

Finally, we have shown that the Gibbs-Duhem methodology presented here can be used to analyze the impact that a change in the value of certain parameter of the potential has on a certain coexistence line. This is very useful since it shows the direction in which the parameter must be changed to bring the coexistence line of the model in better agreement with the coexistence line of real water.[117] The introduction of flexibility, polarizability, quantum effects, modifications of the repulsive part has been undertaken by a number of researchers[118,22,119–124,51,125] and it remains to be seen which of these factors, when included, may lead to a significant improvement in the description of the phase diagram.

ACKNOWLEDGMENTS

This project was financed by Grant Nos. FIS2004-06227-C02-02 and FIS2004-02954-C03-02 of Dirección General de Investigación. A Formación del Profesorado Universitario Ph.D. grant (E.S.) is gratefully acknowledged.

[1] P. Ball, *Life's Matrix. A Biography of Water* (University of California Press, Berkeley, 2001).
[2] J. P. Poirier, Nature (London) **299**, 683 (1982).
[3] J. A. Barker and R. O. Watts, Chem. Phys. Lett. **3**, 144 (1969).
[4] A. Rahman and F. H. Stillinger, J. Chem. Phys. **55**, 3336 (1971).
[5] R. M. Lynden-Bell, J. C. Rasaiah, and J. P. Noworyta, Pure Appl. Chem. **73**, 1721 (2001).
[6] K. M. ABerg, A. P. Lyubartsev, S. P. Jacobsson, and A. Laaksonen, J. Chem. Phys. **120**, 3770 (2004).
[7] M. Ferrario, G. Ciccotti, E. Spohr, T. Cartailler, and P. Turq, J. Chem. Phys. **117**, 4947 (2002).
[8] D. Paschek, J. Chem. Phys. **120**, 6674 (2004).
[9] C. R. W. Guimaraes, G. Barreiro, C. A. F. de Oliveria, and R. B. de Alencastro, Braz. J. Phys. **34**, 126 (2004).
[10] B. Guillot, J. Mol. Liq. **101**, 219 (2002).
[11] H. J. C. Berendsen, J. P. M. Postma, W. F. van Gunsteren, and J. Hermans, in *Intermolecular Forces*, edited by B. Pullman (Reidel, Dordrecht, 1982), p. 331.
[12] H. J. C. Berendsen, J. R. Grigera, and T. P. Straatsma, J. Phys. Chem. **91**, 6269 (1987).
[13] W. L. Jorgensen, J. Chandrasekhar, J. D. Madura, R. W. Impey, and M. L. Klein, J. Chem. Phys. **79**, 926 (1983).

[14]M. W. Mahoney and W. L. Jorgensen, J. Chem. Phys. **112**, 8910 (2000).
[15]H. W. Horn, W. C. Swope, J. W. Pitera, J. D. Madura, T. J. Dick, G. L. Hura, and T. Head-Gordon, J. Chem. Phys. **120**, 9665 (2004).
[16]A. K. Soper, Chem. Phys. **258**, 121 (2000).
[17]T. Head-Gordon and G. Hura, Chem. Rev. (Washington, D.C.) **102**, 2651 (2002).
[18]Y. Guissani and B. Guillot, J. Chem. Phys. **98**, 8221 (1993).
[19]J. Alejandre, D. Tildesley, and G. A. Chapela, J. Chem. Phys. **102**, 4574 (1995).
[20]J. Marti, J. A. Padro, and E. Guardia, J. Chem. Phys. **105**, 639 (1996).
[21]G. C. Boulougouris, I. G. Economou, and D. N. Theodorou, J. Phys. Chem. B **102**, 1029 (1998).
[22]J. R. Errington and A. Z. Panagiotopoulos, J. Phys. Chem. B **102**, 7470 (1998).
[23]M. Lisal, W. R. Smith, and I. Nezbeda, Fluid Phase Equilib. **181**, 127 (2001).
[24]A. G. Kalinichev, Reviews in Mineralogy Geochemistry **42**, 83 (2001).
[25]C. Nieto-Draghi, J. Bonet-Avalos, and B. Rousseau, J. Chem. Phys. **118**, 7954 (1996).
[26]A. D. Mackie, J. Hernandez-Cobos, and L. F. Vega, J. Chem. Phys. **111**, 2103 (1999).
[27]O. Mishima, L. D. Calvert, and E. Whalley, Nature (London) **310**, 393 (1984).
[28]O. Mishima, L. Calvert, and E. Whalley, Nature (London) **314**, 76 (1985).
[29]O. Mishima, J. Chem. Phys. **100**, 5910 (1994).
[30]M.-C. Bellissent-Funel, Europhys. Lett. **42**, 161 (1998).
[31]R. J. Speedy, P. G. Debenedetti, R. S. Smith, C. Huang, and B. D. Kay, J. Chem. Phys. **105**, 240 (1996).
[32]O. Mishima and H. E. Stanley, Nature (London) **396**, 329 (1998).
[33]P. G. Debenedetti, J. Phys.: Condens. Matter **15**, R1669 (2003).
[34]T. Loerting, C. Salzmann, I. Kohl, E. Mayer, and A. Hallbrucker, Phys. Chem. Chem. Phys. **3**, 5355 (2001).
[35]C. A. Angell, D. R. MacFarlane, and M. Oguni, Ann. N.Y. Acad. Sci. **484**, 241 (1986).
[36]P. Jenniskens, D. F. Blake, M. A. Wilson, and A. Pohorille, Astrophys. J. **455**, 389 (1995).
[37]J. S. Tse and M. L. Klein, Phys. Rev. Lett. **58**, 1672 (1987).
[38]J. S. Tse, J. Chem. Phys. **96**, 5482 (1992).
[39]P. H. Poole, F. Sciortino, U. Essmann, and H. E. Stanley, Nature (London) **360**, 324 (1992).
[40]H. Tanaka, J. Chem. Phys. **105**, 5099 (1996).
[41]I. Okabe, H. Tanaka, and K. Nakanishi, Phys. Rev. E **53**, 2638 (1996).
[42]B. Guillot and Y. Guissani, J. Chem. Phys. **119**, 11740 (2003).
[43]R. Martoňák, D. Donadio, and M. Parrinello, Phys. Rev. Lett. **92**, 225702 (2004).
[44]M. D. Morse and S. A. Rice, J. Chem. Phys. **76**, 650 (1982).
[45]I. Borzsak and P. T. Cummings, Chem. Phys. Lett. **300**, 359 (1999).
[46]R. B. Ayala and V. Tchijov, Can. J. Phys. **81**, 11 (2003).
[47]G. C. Leon, S. R. Romo, and V. Tchijov, J. Phys. Chem. Solids **63**, 843 (2002).
[48]S. W. Rick and A. D. J. Haymet, J. Chem. Phys. **118**, 9291 (2003).
[49]G. T. Gao, X. C. Zeng, and H. Tanaka, J. Chem. Phys. **112**, 8534 (2000).
[50]M. J. Vlot, J. Huinink, and J. P. van der Eerden, J. Chem. Phys. **110**, 55 (1999).
[51]H. Nada and J. P. J. M. van der Eerden, J. Chem. Phys. **118**, 7401 (2003).
[52]L. A. Báez and P. Clancy, J. Chem. Phys. **103**, 9744 (1995).
[53]B. W. Arbuckle and P. Clancy, J. Chem. Phys. **116**, 5090 (2002).
[54]T. Bryk and A. D. J. Haymet, J. Chem. Phys. **117**, 10258 (2002).
[55]T. Bryk and A. D. J. Haymet, Mol. Simul. **30**, 131 (2004).
[56]H.-J. Woo and P. A. Monson, J. Chem. Phys. **118**, 7005 (2003).
[57]P. W. Bridgman, Proc. Am. Acad. Arts Sci. **47**, 441 (1912).
[58]V. F. Petrenko and R. W. Whitworth, *Physics of Ice* (Oxford University Press, New York, 1999).
[59]B. Kamb, in *Structural Chemistry and Molecular Biology*, edited by A. Rich and N. Davidson (Freeman, San Francisco, 1968), pp. 507–542.
[60]D. Eisenberg and W. Kauzmann, *The Structure and Properties of Water* (Oxford University Press, London, 1969).
[61]C. Lobban, J. L. Finney, and W. F. Kuhs, Nature (London) **391**, 268 (1998).
[62]M. M. Koza, H. Schober, T. Hansen, A. Tölle, and F. Fujara, Phys. Rev. Lett. **84**, 4112 (2000).
[63]G. P. Johari, J. Chem. Phys. **118**, 242 (2003).
[64]E. Sanz, C. Vega, J. L. F. Abascal, and L. G. MacDowell, Phys. Rev. Lett. **92**, 255701 (2004).
[65]E. Sanz, C. Vega, J. L. F. Abascal, and L. G. MacDowell, J. Chem. Phys. **121**, 1165 (2004).
[66]L. G. MacDowell, E. Sanz, C. Vega, and L. F. Abascal, J. Chem. Phys. **121**, 10145 (2004).
[67]C. McBride, C. Vega, E. Sanz, and J. L. F. Abascal, J. Chem. Phys. **121**, 11907 (2004).
[68]C. McBride, C. Vega, E. Sanz, L. G. MacDowell, and J. L. F. Abascal, Mol. Phys. **103**, 1 (2005).
[69]D. Frenkel and A. J. C. Ladd, J. Chem. Phys. **81**, 3188 (1984).
[70]C. Vega and P. A. Monson, J. Chem. Phys. **109**, 9938 (1998).
[71]C. Lobban, J. L. Finney, and W. F. Kuhs, J. Chem. Phys. **112**, 7169 (2000).
[72]R. Howe and R. W. Whitworth, J. Chem. Phys. **86**, 6443 (1987).
[73]M. Parrinello and A. Rahman, J. Appl. Phys. **52**, 7182 (1981).
[74]D. A. Kofke, J. Chem. Phys. **98**, 4149 (1993).
[75]D. A. Kofke, Mol. Phys. **78**, 1331 (1993).
[76]R. Agrawal and D. A. Kofke, Mol. Phys. **85**, 43 (1995).
[77]D. A. Kofke, in *Monte Carlo Methods in Chemical Physics*, edited by D. M. Ferguson, J. I. Siepmann, and D. G. Truhlar (Wiley, New York, 1998), Vol. 105, p. 405.
[78]P. A. Monson and D. A. Kofke, in *Advances in Chemical Physics*, edited by I. Prigogine and S. A. Rice (Wiley, New York, 2000), Vol. 115, p. 113.
[79]D. A. Kofke, Phys. Rev. Lett. **74**, 122 (1995).
[80]R. Agrawal and D. A. Kofke, Mol. Phys. **85**, 23 (1995).
[81]P. J. Camp, C. P. Mason, M. P. Allen, A. A. Khare, and D. A. Kofke, J. Chem. Phys. **105**, 2837 (1996).
[82]P. Bolhuis and D. Frenkel, J. Chem. Phys. **106**, 666 (1997).
[83]E. de Miguel and E. M. del Rio, J. Chem. Phys. **115**, 9072 (2001).
[84]J. D. Bernal and R. H. Fowler, J. Chem. Phys. **1**, 515 (1933).
[85]F. H. Stillinger and A. Rahman, J. Chem. Phys. **60**, 1545 (1974).
[86]D. van der Spoel, P. J. van Maaren, and H. J. C. Berendsen, J. Chem. Phys. **108**, 10220 (1998).
[87]M. Lísal, J. Kolafa, and I. Nezbeda, J. Chem. Phys. **117**, 8892 (2002).
[88]S. W. Rick, J. Chem. Phys. **120**, 6085 (2004).
[89]D. J. Price and C. L. Brooks, J. Chem. Phys. **121**, 10096 (2004).
[90]H. Yu and W. F. van Gunsteren, J. Chem. Phys. **121**, 9549 (2004).
[91]D. Frenkel and B. Smit, *Understanding Molecular Simulation* (Academic, London, 1996).
[92]S. Yashonath and C. N. R. Rao, Mol. Phys. **54**, 245 (1985).
[93]V. Buch, P. Sandler, and J. Sadlej, J. Phys. Chem. B **102**, 8641 (1998).
[94]L. Pauling, J. Am. Chem. Soc. **57**, 2680 (1935).
[95]J. A. Hayward and J. R. Reimers, J. Chem. Phys. **106**, 1518 (1997).
[96]C. Lobban, J. L. Finney, and W. F. Kuhs, J. Chem. Phys. **117**, 3928 (2002).
[97]Y. Koyama, H. Tanaka, G. Gao, and X. C. Zeng, J. Chem. Phys. **121**, 7926 (2004).
[98]A. Z. Panagiotopoulos, Mol. Phys. **61**, 813 (1987).
[99]M. Lisal, I. Nezbeda, and W. R. Smith, J. Phys. Chem. B **108**, 7412 (2004).
[100]O. Matsuoka, E. Clementi, and M. Yoshimine, J. Chem. Phys. **64**, 1351 (1976).
[101]J. L. Finney, J. E. Quinn, and J. O. Baum, in *Water Science Reviews 1*, edited by F. Franks (Cambridge University Press, Cambridge, 1985).
[102]J. L. Finney, J. Mol. Liq. **90**, 303 (2001).
[103]N. A. Tikhomirova and S. M. Stishov, Sov. Phys. JETP **43**, 2321 (1962).
[104]S. M. Stishov, in *New Kinds of Phase Transitions: Transformations in Disordered Substances*, edited by V. V. Brazhkin, S. V. Buldyrev, V. N. Ryzhov, and H. E. Stanley (Kluwer Academic, Dordrecht, 2002), pp. 3–14.
[105]J. Badro, P. Gillet, and J. L. Barrat, Europhys. Lett. **42**, 643 (1998).
[106]A. Trave, P. Tangney, S. Scandolo, A. Pasquarello, and R. Car, Phys. Rev. Lett. **89**, 245504 (2002).
[107]F. H. Stillinger and P. G. Debenedetti, Biophys. Chem. **105**, 211 (2003).
[108]S. J. Henderson and R. J. Speedy, J. Phys. Chem. **91**, 3069 (1987).
[109]I. M. Svishchev and P. G. Kusalik, Phys. Rev. Lett. **73**, 975 (1994).
[110]M. Matsumoto, S. Saito, and I. Ohmine, Nature (London) **416**, 409 (2002).
[111]R. Radhakrishnan and B. Trout, J. Am. Chem. Soc. **125**, 7743 (2003).
[112]J. P. v. d. E. H. Nada and Y. Furukawa, J. Cryst. Growth **266**, 297 (2004).
[113]H. Tanaka and K. Koga, in *Water in Confining Geometries*, edited by V. Buch and J. P. Devlin (Springer, New York, 2003), pp. 151–177.
[114]A. Striolo, K. E. Gubbins, A. A. Chialvo, and P. T. Cummings, Mol. Phys. **102**, 243 (2004).
[115]I. Brovchenko, D. Paschek, and A. Geiger, J. Chem. Phys. **113**, 5026

(2000).
[116] F. Sciortino, U. Essmann, H. E. Stanley, M. Hemmati, J. Shao, G. H. Wolf, and C. A. Angell, J. Chem. Phys. **52**, 6484 (1995).
[117] M. Z. Hernandes, J. B. P. da Silva, and R. L. Longo, J. Comput. Chem. **24**, 973 (2003).
[118] K. Laasonen, M. Sprik, M. Parrinello, and R. Car, J. Chem. Phys. **99**, 9080 (1993).
[119] B. Chen, J. Xing, and J. I. Siepmann, J. Phys. Chem. B **104**, 2378 (2000).
[120] B. Guillot and Y. Guissani, J. Chem. Phys. **114**, 6720 (2001).
[121] P. L. Geissler, C. Dellago, D. Chandler, J. Hutter, and M. Parrinello, Science **291**, 2121 (2001).
[122] H. A. Stern and B. J. Berne, J. Chem. Phys. **115**, 7622 (2001).
[123] M. Mahoney and W. L. Jorgensen, J. Chem. Phys. **115**, 10758 (2001).
[124] H. Yu, T. Hansson, and W. F. van Gunsteren, J. Chem. Phys. **118**, 221 (2003).
[125] I. Nezbeda, J. Mol. Liq. **73**, 317 (1997).